

Polymerization kinetics of n-butyl cyanoacrylate glues used for vascular embolization

Y. J. Li^a, D. Barthès-Biesel^a, A.-V. Salsac^{a,*}

^a*Biomechanics and Bioengineering Laboratory (UMR CNRS 7338), Université de technologie de Compiègne - CNRS, Sorbonne universités, CS 60319, 60203 Compiègne, France*

Abstract

Vascular embolization is a minimally invasive treatment used for the management of vascular malformations and tumors. It is carried out under X-ray by navigating a microcatheter into the targeted blood vessel, through which embolic agents are delivered to occlude the vessels. Cyanoacrylate liquid glues have been widely used for vascular embolization owing to their low viscosity, rapid polymerization/solidification rate, good penetration ability and low tissue toxicity. The objective of this study is to quantitatively investigate the physical properties of two n-butyl cyanoacrylate (nBCA) glues (Glubran 2 and Histoacryl) mixed with an iodized oil (Lipiodol) at various concentrations. We show that an homogeneous solution results from the mixing of the glue and Lipiodol, and that the viscosity, density and interfacial tension of the mixture increase with the proportion in Lipiodol. We have designed a new experimental setup to systemically characterize the polymerization kinetics of a glue mixture upon contact with an ionic solution. We observe that the whole polymerization process includes two phases: an interfacial polymerization that takes place at the interface as soon as the two liquids are in contact with a characteristic time scale of the order of the minute; a volumetric polymerization during which a reaction front propagates within the mixture bulk with a characteristic time scale of the order of tens of minutes. The polymerization rate, front propagation speed and volume reduction increase with the glue concentrations. It is the first time that such comprehensive results are obtained on liquid embolic agents.

*Corresponding author

Email address: anne-virginie.salsac@utc.fr (A.-V. Salsac)

Keywords: Vascular embolization, Interfacial polymerization, Volumetric polymerization, Glubran 2, Histoacryl

1. Introduction

Vascular embolization is a minimally invasive treatment used to selectively reduce or stop the blood supply to specific parts of the body. It consists of injecting liquid embolic agents, typically glues, which polymerize and solidify quickly upon contact with blood and thus occlude the vessels. It is carried out under X-ray by navigating a guidewire and a catheter into the targeted blood vessel, through which the embolic agents are delivered. The technique is widely used for the management of arteriovenous malformations [1], gastric varices [2], tumors [3, 4] or hemorrhage upon vessel rupture, with new applications regularly appearing in medical practice.

Typical liquid embolic agents are cyanoacrylates glues which are well suited for vascular embolization: they have a low viscosity, short polymerization/solidification time and low tissue toxicity [5]. This latter property has led to the development of cyanoacrylate biodegradable nanometric drug carriers [6, 7, 8] and of cyanoacrylate biocompatible nanofibers that have a wide range of applications [9]. The monomeric cyanoacrylate structure consists of a double-carbon ethylene group with two reactive electro-withdrawing functions (cyano $-CN$ and ester $-COOR$). Upon reaction with anions or radicals, a reactive carbanion or radical forms, which reacts with further monomers to finally form a polymer (Figure 1). There are presently two commonly used embolic glues: the first one is n-butyl cyanoacrylate (nBCA), available under the trademark Histoacryl (B. Braun, Melsungen, Germany). The other one, available under the trademark Glubran 2 (GEM, Viareggio, Italy), is composed of nBCA mixed with a co-monomer: metacryloxysulpholane (MS). The addition of MS allows to lower the polymerization temperature to about 45 °C. To make the embolic agent radio-opaque and enable its detection after injection in the vessels, cyanoacrylate glues are mixed with a contrast agent, typically an iodized poppy seed oil such as Lipiodol (Laboratoire Guerbet, Aulnay-sous-Bois, France). The volume ratio of cyanoacrylate glue to iodized oil is usually varied between 1:1 and 1:5 depending on the vessel diameter, desired penetration distance and blood velocity.

When the glue-oil mixture is injected in the blood stream, it tends to polymerize because of the presence of ions in the plasma. The polymerization kinetics thus play an essential role in the control of the injection and

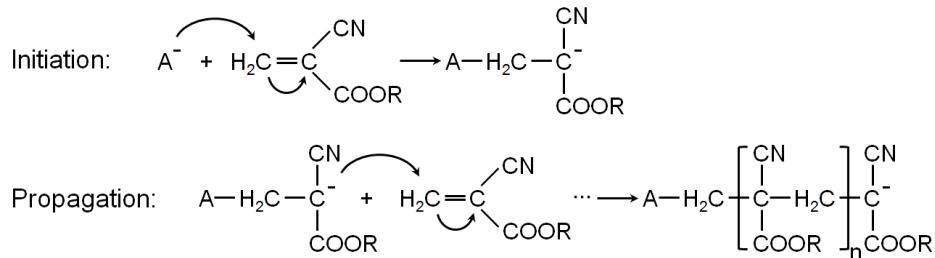


Figure 1: Initiation and propagation steps in anionic polymerization of alkyl (R) cyanoacrylate initiated by anions (A^-).

subsequent flow occlusion processes. The usual empirical technique to evaluate the polymerization time of glue-oil mixtures consists of dropping a small quantity of mixture onto a plasma or citrated blood substrate and visualizing its change in opacity (whitening) [10, 11]. This technique is qualitative: the change in opacity depends on the volume of deposited mixture and the ending criteria of polymerization are not precisely defined. As the mixture viscosity is low, the thickness of deposited volume is small. Consequently the technique essentially provides information on the initial stage of polymerization inside a thin sheet of glue mixture in contact with ions. Using this technique, the initial polymerization time for mixtures of nBCA and Lipiodol has been evaluated between 5 s and 10 s, but no study ever investigated Glubran 2.

Presently, we do not know how fast the polymerization reaction propagates inside a finite volume of glue mixture, although this information is crucial: the typical transversal dimension of an injected glue mixture volume is dictated by the size of the catheter and is thus of the order of $\sim 1 - 5$ mm depending on the injection conditions [12, 13]. There is therefore the need for a quantitative systematic study of the reactions that occur at the glue-blood interface and within the glue mixture both for nBCA and nBCA-MS glues.

The objective of the present study is to quantitatively characterize the polymerization of glue-Lipiodol mixtures upon contact with an ionic solution. We have thus designed a novel experimental setup that enables to investigate both interfacial and volumetric aspects of the polymerization of glue-oil mixtures in contact with an ionic solution. The basic idea is to suddenly create a well-defined interface between the glue and the ionic solution. The aim is then to study the polymerization reaction within the glue volume and provide information on its propagation. With the same set-up, we can also

evaluate the initiation of the reaction by studying the polymerization of a thin film that is a few microns in thickness. In the following, the former will be referred to as "volumetric polymerization", while the latter will be called "interfacial polymerization". We have thus conducted a systematic, well-controlled characterization of the polymerization process of mixtures of cyanoacrylate glues and Lipiodol as a function of their concentration in glue, and compared results between Glubran 2 (nBCA-MS glue) and Histoacryl (pure nBCA glue). We show that if the initial interfacial polymerization is fast, such is not the case for the reaction inside the volume of the glue mixture, which can remain in liquid state for a long time (over one hour). The results thus provide crucial information to interventional radiologists, that will help them understand and control the glue behavior after injection to achieve a safe and permanent obliteration of the vessels.

The paper is organized as follows. After having described how to prepare the glue mixture and ionic solution, we detail the experimental technique used to enquire on the miscibility of glue and Lipiodol, and end the material and method section (§2) with the description of the experimental setup designed to characterize the polymerization process. The result section (§3) is structured in 3 subsections providing a summary of the main results obtained on the glue miscibility, volumetric polymerization and interfacial polymerization. The implication of the results are discussed in §4.

2. Materials and methods

2.1. Preparation and characterization of the glue mixture and ionic solution

Glubran 2-Lipiodol (G-L) and Histoacryl-Lipiodol (H-L) mixtures are prepared by means of a female luer connector attached to two 1-ml syringes, one loaded with glue and the other with Lipiodol. Both glues are stored in sealed containers at 4 °C and left at room temperature 2 minutes before use. Lipiodol is, however, stored at room temperature. A 0.2 ml total volume of glue and Lipiodol is mixed with volume ratios 1:0, 3:1 and 1:1, corresponding to glue concentrations $C_G = 100\%$, 75% and 50%, respectively. The mixing process consists of manually passing the liquids from one syringe to the other several times at a high frequency (about 150 times in 90 seconds). All the experiments are conducted at 21 °C.

Blood naturally consists of a suspension of cells in plasma, which is made of proteins, metallic ions (8%) and water (92%). The objective of the present

Solute	Quantity
NaCl	7.19 g
KCl	0.2 g
KH ₂ PO ₄	0.2 g
Na ₂ HPO ₄ ·12H ₂ O	2.864 g
Glucose	0.8 g
Glycerol	320 ml
Deionized water	680 ml

Table 1: Composition of 1 L of ionic solution.

study is to determine the influence of the blood anions on the glue polymerization. An ionic solution has thus been used to initiate the reaction. It has the same ionic composition and $pH = 7.3 \pm 0.1$ as blood (see composition in Table 1). To match the solution viscosity to that of blood, some glycerol is incorporated into it. The ionic solution has then a density of 1094.5 kg/m^3 and dynamic viscosity of $3.8 \times 10^{-3} \text{ Pa}\cdot\text{s}$ at $21 \text{ }^\circ\text{C}$. The interfacial tension is slightly higher than that of blood ($69 \times 10^{-3} \text{ N/m}$ vs $50 \times 10^{-3} \text{ N/m}$ for blood), but this should not affect the present results [13].

The physical properties of G-L mixtures had to be characterized first, as no information is available in the literature. The viscosity was measured with a rheometer (RheoStress1, Thermo Haake, Germany) in cone-plane configuration (diameter 60 mm, angle 0.5°). The density of the solutions was determined with a digital density-meter (DMA 45, Anton Paar, Austria) with an accuracy of $\pm 10^{-4} \text{ g/cm}^3$ (manufacturer values). For pure Glubran 2, the density was determined by weighting a sample of known volume with a high precision scale (Precisa 92SM-202A, Elsiechrom, Sweden) having an accuracy of $\pm 10^{-4} \text{ g}$. The risk was indeed too high to clog the internal tube of the density-meter with Glubran 2. The viscosity μ and density ρ are given at $21 \text{ }^\circ\text{C}$ in Figure 2 as a function of glue concentration. The results indicated for Histoacryl in Figure 2 have been obtained by interpolating the values of Bracard *et al.* [14] for the temperature of $21 \text{ }^\circ\text{C}$. It appears that the two glue mixtures have almost the same viscosity and density.

The interfacial tension γ between the glue mixtures and purified water (Milli-Q, Merck Millipore, USA) was measured at $21 \text{ }^\circ\text{C}$ with the pendant drop technique (Drop Shape Analyzer DSA10, Kruss, Germany). The results are shown in Figure 3. It was, however, not possible to use this technique

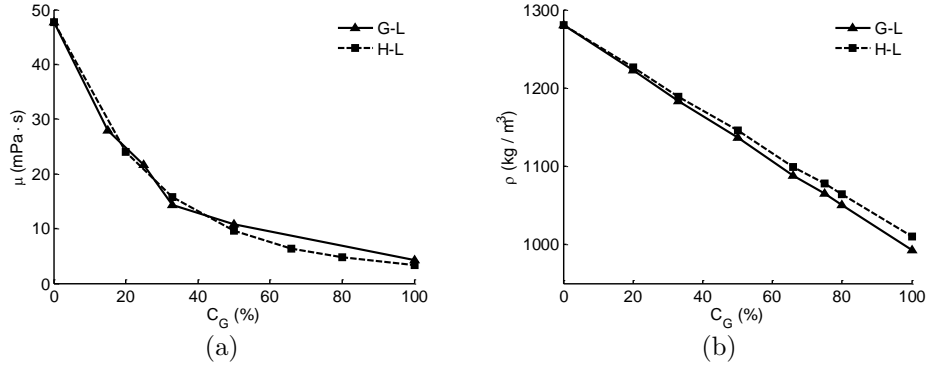


Figure 2: Viscosity μ (a) and density ρ (b) of G-L and H-L mixtures at 21 °C [15]. The viscosity of H-L mixtures is inferred from Bracard *et al.* [14].

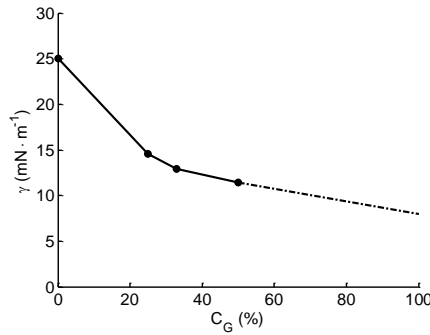


Figure 3: Interfacial tension γ between purified water and G-L mixtures at 21 °C [15]. The dashed line is an extrapolation.

for glue concentrations larger than 50%, because polymerization occurred immediately after contact with water. Since the γ vs C_G curve seems to level off, we have extrapolated linearly the curve for $C_G > 50\%$.

2.2. Miscibility of nBCA glue and Lipiodol

The miscibility of nBCA glues with Lipiodol is assessed in a diffusion device, consisting of a parallelepipedic transparent cup (UV cuvette, Brand, Germany), as shown in Figure 4a. The bottom of the cup is first filled with $\sim 135 \mu\text{L}$ of Lipiodol (translucent, pale yellow). Then $\sim 150 \mu\text{L}$ of Histoacryl (translucent, blue) is carefully poured onto the Lipiodol, taking care that minimum mixing takes place during the procedure. The cup is then closed

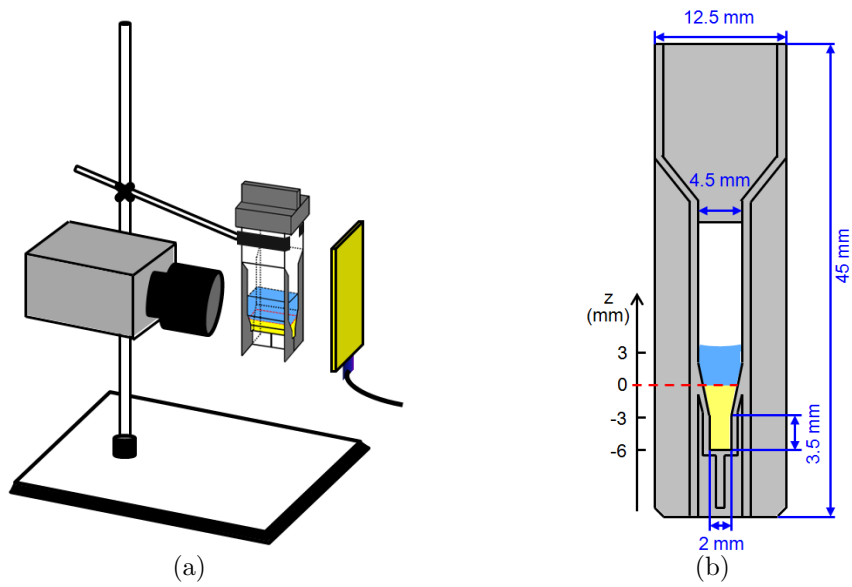


Figure 4: Experimental setup to study the miscibility of glue and Lipiodol (at the top and bottom of the cup, respectively). (a) The two fluids are put in contact in a cup and the change in opacity of the system is monitored by a camera with a back-light device. (b) Detail of the cup cross-section.

hermetically to limit evaporation, and placed vertically in front of a high-speed camera (SA3, Photron, USA). An optical fibre panel (Schott-Fostec, LLC, USA) is used as back illumination source (Figure 4a). The diffusion process between the two liquids is captured by the camera at the rate of one frame every 30 seconds over 2 days. The recorded images are encoded in 16 bits which are converted to 8 bits in the measurement process, providing 256 possible shades of grey: 0 corresponding to black and 255 to white. The concentration distribution is then assessed from the image grey level distribution G_m . The z -axis is aligned with the tube centerline, the origin $z = 0$ corresponding to the initial position of the glue-Lipiodol interface. Initially, the glue is thus in the $z > 0$ region and Lipiodol in the $z < 0$ region (Figure 4b). The grey levels are measured at 24 test points, equally distributed along the z -axis with a 0.38 mm interval. The value $G_m(z)$ corresponds to the average of G_m within a box of width 1.36 mm and height 0.28 mm centered on each test point. Note that the grey level values are relative and may vary between two experiments, depending on light settings for example. However, the grey level basis is constant during one experiment.

2.3. Characterization of the polymerization process

An experimental setup has been designed to visualize the polymerization of the glue-Lipiodol mixture when it is put in contact with the ionic solution. The principle consists of creating a small well-defined interface between the two fluids and following the propagation of the reaction through the change in opacity of the glue volume.

Specifically, the polymerization reaction is studied under static conditions in a vertical glass micro-tube (internal diameter $D_t = 1.06 \pm 0.01$ mm). First a volume of glue mixture is aspirated into the tube from a small cup placed underneath, by means of a syringe connected to the tube upper end (Figure 5a). The glue cup is replaced by one containing the ionic solution: the glue mixture and ionic solution then come into contact and are aspirated quickly together from the lower tube tip to a static position (Figure 5b). The contact surface between the glue mixture and the ionic solution corresponds to the tube cross section. The polymerization can only propagate from this surface into the glue volume inside the tube. With this device, we have essentially reduced the volume polymerization to a one-dimensional front propagation along the tube axis. A z -axis is defined along the axis of the tube with the origin $z = 0$ corresponding to the position of the interface at the end of the aspiration process, which lasts between 5 and 10 s (Figure 5b). The glue

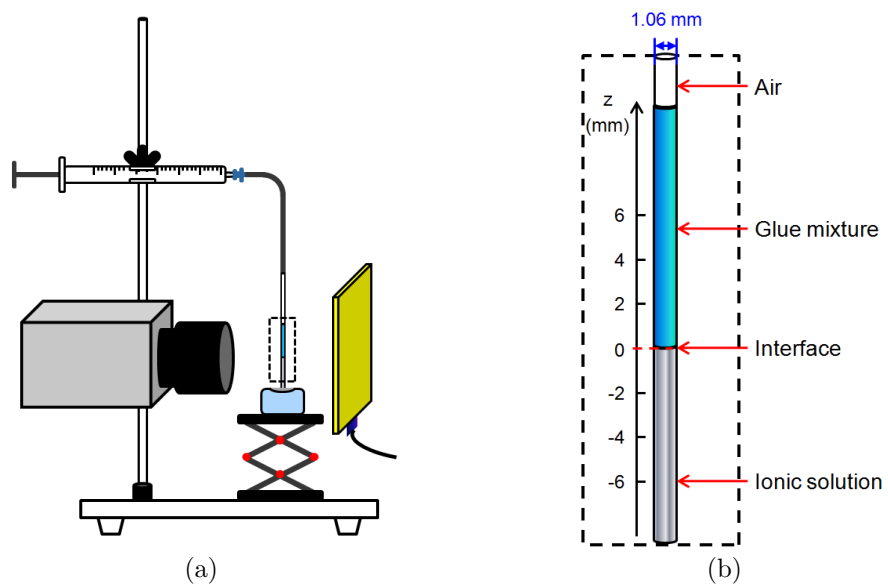


Figure 5: Experimental set-up to study the polymerisation of glue-Lipiodol mixtures in contact with the ionic solution. (a) The two fluids are put in contact in a micro-tube and the change in opacity of the system is monitored by a camera with a back-light device. (b) Detail of the tube.

mixture is initially in the $z > 0$ region and the ionic solution in the $z < 0$ region. The progression of the polymerization reaction is then evaluated from the change in opacity of the glue mixture for different values of z . The image grey level $G_p(z)$ of the fluids is monitored with the imaging system consisting of the high-speed Photron camera coupled to the back illumination source.

The beginning of the polymerization process is continuously recorded at a rate of 50 fps with image resolution 128×1024 pixels² during a maximum recording time of 217.8 s. A time-lapse recording mode is then used to monitor the long time polymerization process with a frame rate of 0.5 fps and image resolution 128×1024 pixels². The total recording time ranges from 90 min to 120 min in the different experiments. In both modes, the shutter time is 0.5 ms. All the experiments are conducted at a controlled room temperature of 21 °C. All the experiments have been repeated between 5 and 10 times for each concentration of Glubran 2 and Histoacryl.

The distance between two contiguous measuring points is $0.5 D_e$, where D_e is the diameter of the liquid region as measured on the image (D_e is slightly smaller than D_t because of optical effects). Grey levels are averaged within boxes of width $0.7 D_e$ and height $0.4 D_e$ centered on each test point.

3. Results

3.1. Miscibility of pure nBCA glue with Lipiodol

Images of a Histoacryl-Lipiodol system at different time intervals are shown in Figure 6. At the beginning of the experiment ($t = 0$ h), the interface ($z = 0$) between the glue (dark) and Lipiodol (clear) is sharp. An interdiffusion process then takes place until a homogeneous mixture is formed at $t = 46$ h. This indicates that nBCA glue and Lipiodol are miscible. Grey level profiles $G_m(z, t)$ along the z -axis at different times are shown in Figure 7. At the beginning of the experiment ($t = 0$ h), $G_m(z, 0)$ is a step function: $G_m(z, 0) = 91$ for $z < 0$ (clear Lipiodol) and $G_m(z, 0) = 27$ for $z > 0$ (dark Histoacryl glue). As nBCA molecules diffuse into Lipiodol, the diffusion front, which corresponds to the position along the z -axis where the grey level begins to decrease, moves downwards. Owing to this process, the grey level profile changes from a step function to a sigmoidal shape. The distance, over which the diffusion front propagates is defined as the diffusion length. It increases with time until the diffusion front reaches the bottom of the cup at $t \sim 17$ h, which corresponds to $z = -6$ mm (Figure 7). Afterwards, the diffusion process continues leading to a further decrease in the grey levels in

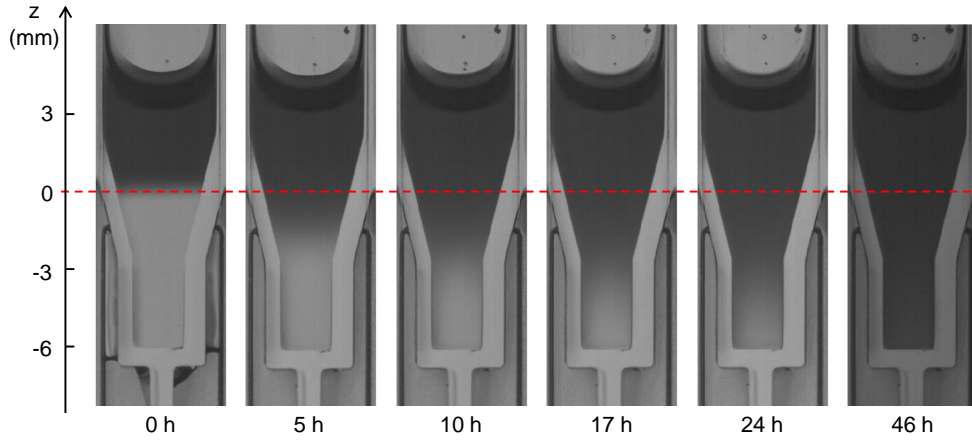


Figure 6: Time evolution of nBCA glue put in contact with Lipiodol: the darkening of the system over time shows that the two liquids are miscible. The dashed line shows the initial position of the interface.

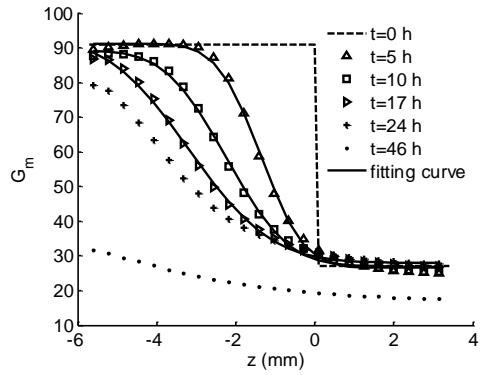


Figure 7: Grey level distribution along the cup axis for different times. The dashed line shows the initial position of the interface. Here, the bottom of the cup is at $z = -6$ mm.

the Lipiodol region ($z < 0$) until a quasi-uniform distribution $G_m(z, \infty)$ is reached.

Since the grey level is proportional to the local concentration at each point in the domain, one can evaluate the diffusion coefficient of nBCA glue in Lipiodol by means of Fick's second law. We consider the one-dimensional case of diffusion, in which two miscible liquids of different concentrations ϕ_1 and ϕ_2 ($\phi_1 > \phi_2$) are initially put in contact at position $z = 0$. We only study the early stages of diffusion, for which the boundary conditions are $\phi(z) \rightarrow \phi_1$ for $z \rightarrow -\infty$ and $\phi(z) \rightarrow \phi_2$ for $z \rightarrow +\infty$. Fick's second law thus leads to the concentration distribution:

$$\phi(z, t) = \frac{\phi_1 + \phi_2}{2} - \frac{\phi_1 - \phi_2}{2} \operatorname{erf}\left(\frac{z}{2\sqrt{Dt}}\right), \quad (1)$$

where $\phi(z, t)$ is the molecular concentration, erf is the error function and D is the diffusion coefficient. As illustrated in Figure 7 for three instants of time, we fit the data with Eq. (1), in which we replace ϕ by G_m , and deduce the value of the diffusion length $2\sqrt{Dt}$ at time t . The diffusion lengths are thus measured by fitting the grey level profiles between 0 and 17 hours. As shown in Figure 8, the square of the diffusion length $4Dt$ is directly proportional to time t . We deduce the value of the diffusion coefficient D and find $D = 2.1 \times 10^{-11} \text{ m}^2/\text{s}$, which is lower than in the case of an aqueous solution ($D \sim 10^{-10} - 10^{-9} \text{ m}^2/\text{s}$). Diffusion of nBCA glues in the Lipiodol oil is thus slower than diffusion in water solutions. A similar diffusion process is obtained for Glubran 2, proving that cyanoacrylate glues are miscible in Lipiodol. We have also checked that a mixture of Glubran and Lipiodol is stable over days: no tendency towards phase separation is observed.

The last point that remains is to estimate how homogeneous the mixture is upon the mixing process. In the present study, the two liquids are mixed by forcing a volume of 0.2 mL through a luer connector of diameter $d_L = 2 \text{ mm}$ every 0.6 s, which corresponds to a shear rate $\dot{\gamma} \sim 200 \text{ s}^{-1}$. The ratio between the convection and diffusion times is thus $Dd_L^2/\dot{\gamma} \sim 10^{-19}$. It follows that the convective mixing procedure is efficient.

3.2. Characterization of the volumetric polymerization

3.2.1. Time-evolution of the glue-mixture opacity

We first analyze the volume polymerization and the propagation of a polymerization front within the glue mixture. Tens of minutes after the end

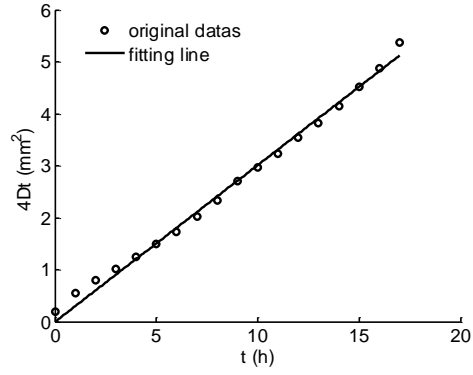


Figure 8: Correlation between the diffusion length and time.

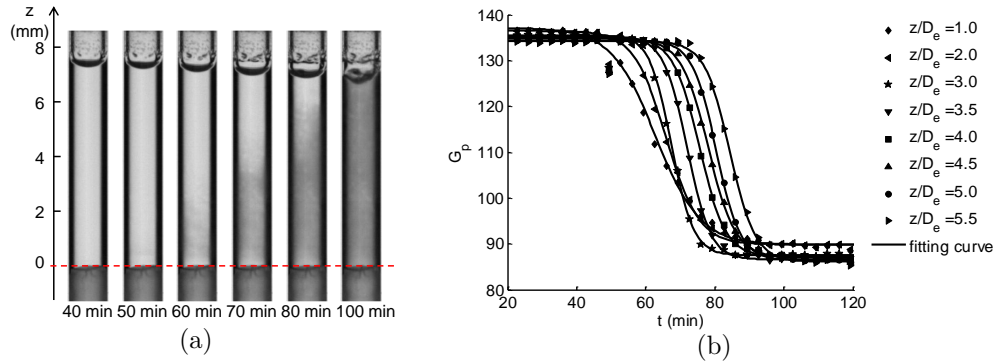


Figure 9: Time evolution of G-L mixture ($C_G = 50\%$) in contact with the ionic solution. (a) The darkening in the glue mixture over time shows the propagation of a polymerization front upwards from the interface. (b) Time evolution of the grey level at different positions in the glue mixture: the symbols correspond to experimental points and the continuous lines to the correlations given by Eq. (2).

of the aspiration, a polymerization front begins to propagate upwards from the interface within the glue mixture (Figure 9a). Since the interface between the mixture and the ionic solution is dark, the grey level change cannot be measured in its vicinity. Measurements are only meaningful for $z \geq D_e/2$. We show in Figure 9b the time evolution of the grey level at different locations along the tube axis for $z/D_e \geq 0.5$. The grey levels decrease from the initial value $G_{p0} \sim 135$ to the asymptotic value $G_{p\infty} \sim 90$. Since the polymerization front propagates from the interface, the further the point location is from the interface, the later the decrease in G_p starts occurring. The fact that the curves get closer to one another as z increases indicates that the propagation velocity increases with z . One can also note that the front becomes steeper.

For every value of z , the curve $G_p(z, t)$ can be fitted with a sigmoid:

$$G_p(z, t) = G_{p0} - \frac{G_{p0} - G_{p\infty}}{1 + \exp\left(-\frac{t - t_{1/2}(z)}{\tau_v}\right)}, \quad (2)$$

where τ_v is the characteristic time and $t_{1/2}(z)$ is the half time, such that $G_p(t_{1/2}) = (G_{p0} + G_{p\infty})/2$. The sigmoidal fitting of the grey level time-evolution works as well as in the example shown in Figure 9 for all the tested concentrations in Glubran 2 and Histoacryl. The time τ_v corresponds to an empirical measure of the time that it takes the polymerization to be completed at position z (based on the grey level in the fluid). Indeed, it takes about $5.9\tau_v$ for the grey level at z to drop from $G_{p0} - 0.05(G_{p0} - G_{p\infty})$ to $G_{p0} - 0.95(G_{p0} - G_{p\infty})$. Figure 10a shows values of τ_v for Histoacryl and Glubran 2. Results are only provided for $C_G = 50\%$ and 75% , as no value could be obtained with sufficient precision for $C_G = 100\%$, the propagation being too fast. In all the cases, τ_v decreases with z , the distance away from the interface. It indicates that the polymerization reaction is slow near the interface during the initiation of the process, and that the reaction accelerates as it propagates away from the interface. A constant value for τ_v is always reached for $z/D_e \geq 2.5$. Figure 10a also shows that the polymerization time decreases significantly when the glue concentration increases. All these results hold both for Glubran 2 and Histoacryl.

Figure 10b shows the half time $t_{1/2}$ for all the glue concentrations, which is a measure of the polymerization front progression. The half time increases slightly with z . It also strongly increases with the Lipiodol concentration, as indicated by the logarithmic scale used to plot the results (Figure 10b). This

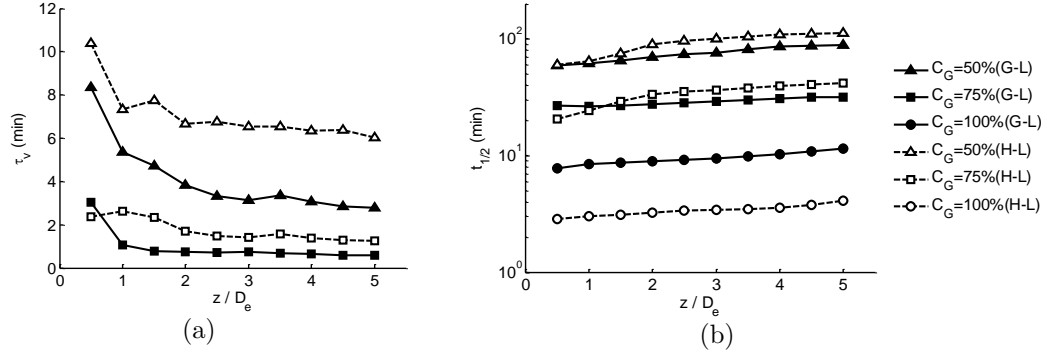


Figure 10: Average characteristic time τ_v (a) and half time $t_{1/2}$ (b) of volume polymerization for different glue concentrations.

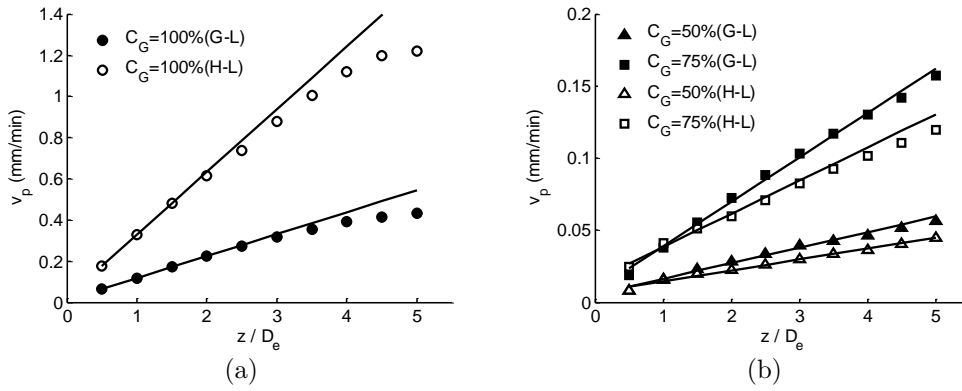


Figure 11: Average propagation velocity v_p for G-L and H-L mixtures at different glue concentrations.

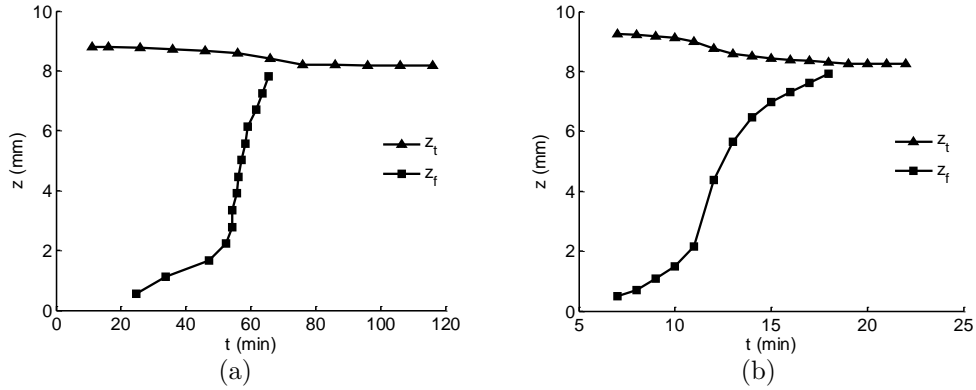


Figure 12: Total length H and position of the beginning of the polymerization front z_f as a function of time for G-L mixtures. (a) $C_G = 50\%$, (b) $C_G = 100\%$.

means that low glue concentration leads to a delay in the propagation of the volumetric polymerization, while this process is very fast for pure glue, as can be surmised from the corresponding small value of $t_{1/2}(z)$. It is also possible to infer the propagation speed of the polymerization front $v_p = z/t_{1/2}(z)$. Since $t_{1/2}(z)$ levels out when z increases, the propagation speed increases almost linearly with z , as shown in Figures 11a-b. The value of v_p increases with C_G and z , which may be due to the fact that the polymerization reaction is exothermic and that the temperature increases along z . The increase of the front velocity with temperature and monomer concentration has been indeed predicted by propagation models [16, 17].

3.2.2. Time-evolution of the glue mixture height

As is apparent in Figure 9a, a change in volume occurs in the glue mixture during volumetric polymerization. To assess the change in volume and see whether it is linked with the chemical reaction, we plot the time-evolution of the coordinate $z_t(t)$ of the top of the glue mixture column in Figure 12, along with the coordinate $z_f(t)$ of the polymerization front. The front position in the glue mixture ($z_f > 0$) is calculated assuming that polymerization begins at the location, where the grey level has decreased by 5% from its initial value, which occurs at time $t_{1/2}(z_f) - 3\tau_v(z_f)$. The results are plotted for two concentrations in Glubran 2 for illustration, similar results having been obtained for Histoacryl. Figure 12 shows that the decrease in glue mixture height can be correlated with the progression of the polymerization inside

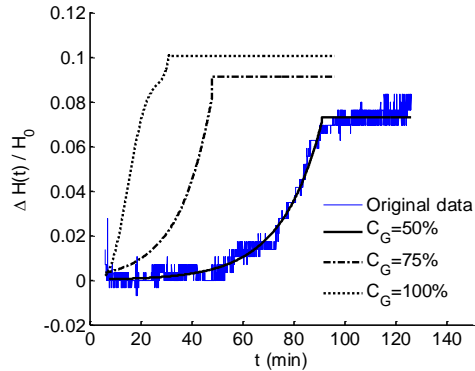


Figure 13: Height reduction at different glue concentrations for G-L mixtures.

the glue: as the polymerization front advances, the coordinate $z_t(t)$ moves down with time. Since the height decrease stops when $z_f \sim z_t$, i.e. when the polymerization front has reached the top of the glue column, it is clear that the two processes, glue polymerization and height reduction, are coupled. Note that the time evolution of $z_f(t)$ again shows the significant acceleration of the polymerization, as it progresses inside the glue.

The decrease in volume means that the density of the glue increases as it polymerizes. It is thus possible to assess the relative increase in density of the polymerized glue from the relative reduction in height:

$$\frac{\rho(t) - \rho_0}{\rho(t)} = \frac{z_t(0) - z_t(t)}{z_t(0)}. \quad (3)$$

The relative height decrease is shown in Figure 13 as a function of time in the case of G-L mixtures. Note that instead of writing $(z_t(0) - z_t(t))/z_t(0)$, we have chosen to denote the relative height reduction as $\Delta H(t)/H_0$ in the figure. It appears that the volume reduction increases with the glue concentration. We also recover the fact that the polymerization speed increases with C_G . The relative density increase is shown in Table 2, where $\Delta\rho$ is the density increase after full polymerization. For G-L mixtures, the higher the glue concentration, the greater the density increase due to polymerization. For H-L mixtures, the density increase is almost independent of concentration, and somewhat larger than for G-L mixtures.

$\Delta\rho/\rho_\infty(\%)$	$C_G = 50\%$	$C_G = 75\%$	$C_G = 100\%$
G-L	7.6 ± 2.2	9.1 ± 1.4	11.1 ± 1.1
H-L	9.8 ± 0.9	10.3 ± 0.8	11.5 ± 0.7

Table 2: Average relative density increase for different glue concentrations.

3.2.3. Microscopic observation of the polymerized glue-mixture

The cross section of the polymerized cylinder of the glue mixture has been observed with a scanning electron microscope (QUANTA FEG 250, FEI, US). Pure Glubran glue ($C_G = 100\%$) exhibits a complex polymerized network (Figure 14a). In the case of a glue-oil mixture, the oil invades all the void space between the polymerized glue, as shown in Figures 14b-c for $C_G = 50\%$. The oil appears as a smooth film from which emerge some glue islets. Since the oil surface is smooth, it is very difficult to get a good SEM definition. The spectroscopy analysis does indeed show the presence of iodine, and thus proves that oil is indeed present (recall that Lipiodol is an iodized oil).

3.3. Characterization of the initiation of the polymerization process: study of interfacial polymerization

Interestingly enough, the tube device can also be used to study the initiation of the polymerization process and its propagation in a thin film of glue. Indeed, as soon as the aspiration is stopped ($t = 0$), the ionic solution begins to darken (Figure 15a), indicating that a polymerization process is occurring. This phenomenon corresponds to the polymerization of a thin film of glue, which is left behind in the $z < 0$ region, during the quick ascension of the glue mixture, when the ionic solution is aspirated. Figure 15b shows the time evolution of the grey level at 3 locations in the ionic solution ($z < 0$) for the measurements of Figure 15a. The initial value of the grey level $G_p(z, 0) \sim 147$ corresponds to that in the ionic solution prior to any polymerization reaction. It then decreases with time, first sharply ($t \leq 50$ s), then slowly for $50 \text{ s} < t < 200$ s and finally very slowly (~ 5 grey level unit change over for 90 min or more). Similar trends are obtained for all the glue concentrations, both in the case of Glubran 2 and Histoacryl. At the end of the experiments, when the polymerization is well completed, the thin film can be removed from the tube (Figure 16a), cut in sections and measured under a microscope (Figure 16b). The thickness of the film has nearly the

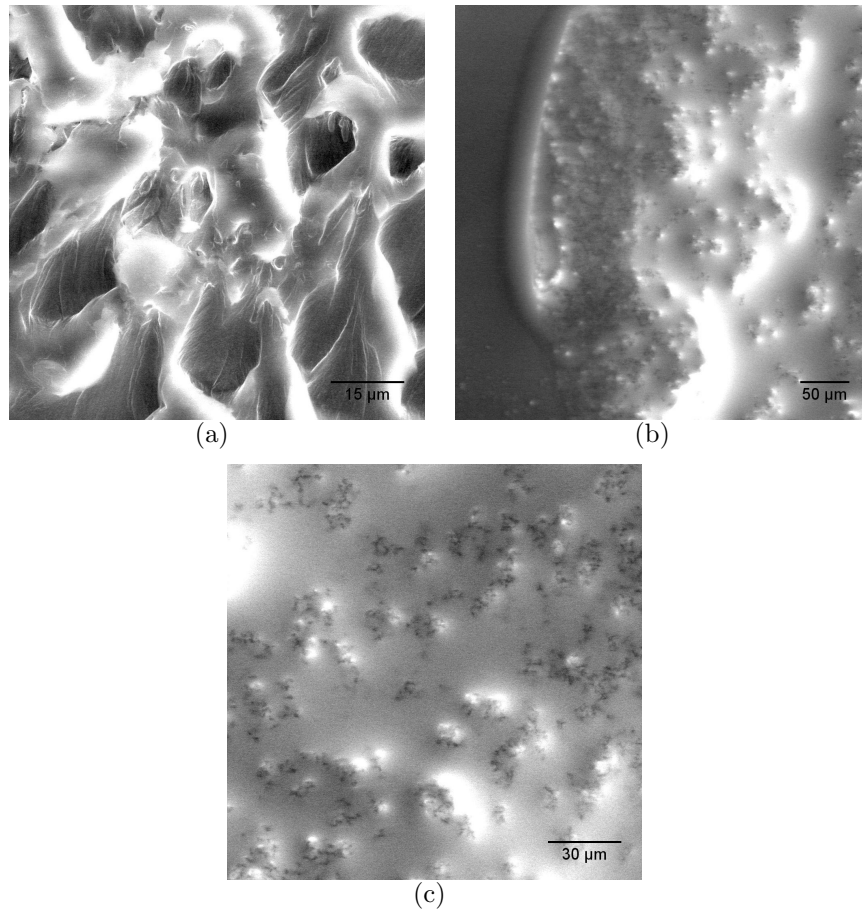


Figure 14: Scanning electron micrograph of the polymerized glue mixture. (a) Pure Glubran $C_G = 100\%$, (b) and (c) Glubran-Lipiodol mixture $C_G = 50\%$: the polymerized glue structure is immersed in oil.

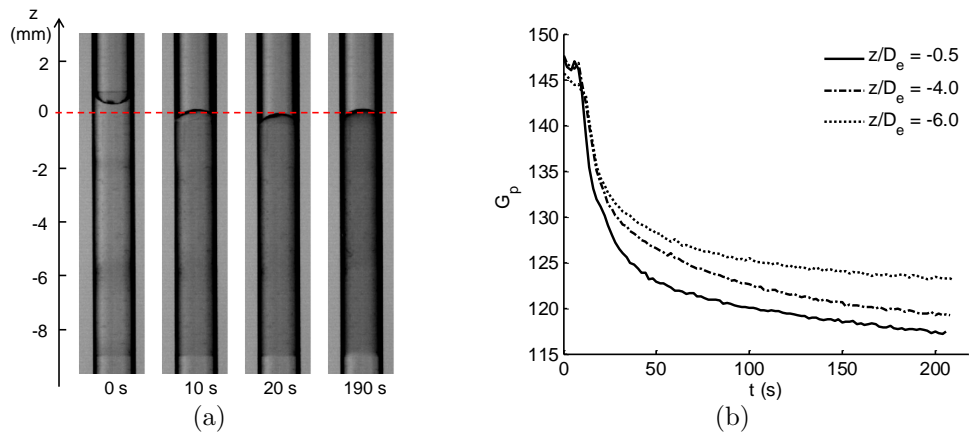


Figure 15: Change in opacity observed in the ionic solution in the case of a G-L mixture ($C_G = 50\%$). (a) Darkening in the ionic solution revealing a polymerization of the G-L film left behind on the tube wall. (b) Grey level time evolution at different positions within the ionic solution.

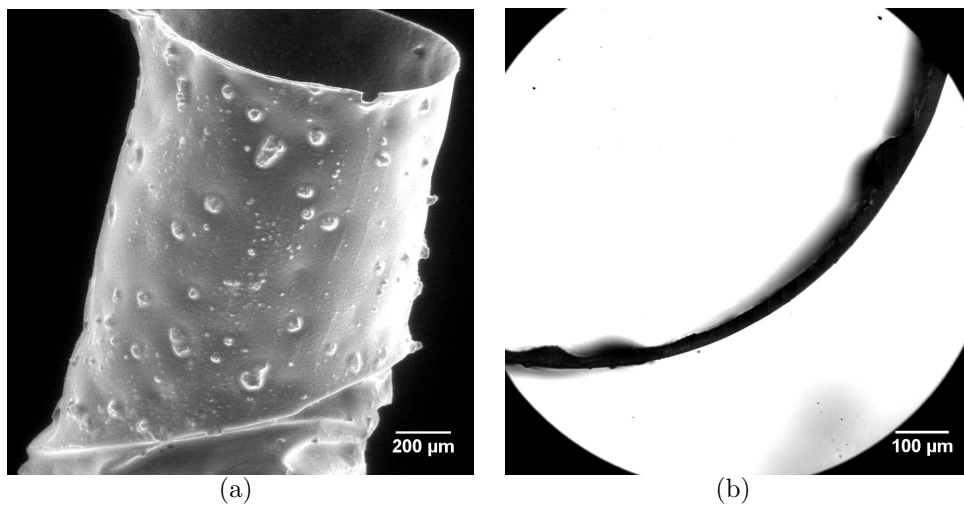


Figure 16: G-L mixture ($C_G = 50\%$): (a) Scanning electron micrograph of a G-L film removed from the tube, (b) optical micrograph of a film section.

τ_f (s)	$C_G = 50\%$	$C_G = 75\%$	$C_G = 100\%$
G-L	116 ± 8	79 ± 11	54 ± 9
H-L	86 ± 9	66 ± 13	41 ± 3

Table 3: Average characteristic times τ_f for which 90% of film polymerization has occurred. Results are for Glubran-Lipiodol and Histoacryl-Lipiodol mixtures, with different glue concentrations.

same value $e = 24 \pm 2 \mu\text{m}$ for all glue concentrations. The theoretical value of e can be estimated using Bretherton's theory [18]:

$$e = \alpha \frac{D_t}{2} (\mu V / \gamma)^{2/3}, \quad (4)$$

where D_t is the internal tube diameter and V is the ascending velocity during the aspiration phase. The factor α takes values between 1.34 (in the case of a clean interface) and 3.37 (in the case where Marangoni effects have the most important effect due to the presence of surfactants) [19]. Using the results of section 2.1 and $V \sim 3 \text{ mm/s}$, we find $e \sim 14 - 35 \mu\text{m}$ for all the glue concentrations. The experimental value that we have measured falls within those limits, which is satisfying knowing that the film is presently generated under the combined effects of flow and polymerization.

The time evolution of the grey levels measured in the film (e.g. Figure 15b) can be used to assess the early stages of polymerization in a thin film. As it is not possible to fit the time-evolution curves with a simple exponential curve, we define the time τ_f as the time for which the grey level has decreased by 90% in the first 200 s:

$$G_p(z, \tau_f) = G_p(z, 0) - 0.9[G_p(z, 0) - G_p(z, 200)]. \quad (5)$$

For all the glue concentrations, we find that τ_f decreases slightly when z decreases, a result which can be inferred from Figure 15b: this effect is due to gravity-induced film thinning. To exclude a possible influence of gravity, we thus consider the values of τ_f obtained for $z/D_e \in [-1, -3]$, a location where the film thickness has roughly the value given by Eq. (4). The average values of the characteristic time τ_f are shown in Table 3 for the different glue mixtures. In all the cases, τ_f is of the order of 1 to 2 min, which is much shorter than the propagation times which were measured for volumetric polymerization in section 3.2.1. This can be explained by the fact that the film

interface between the glue mixture and the ionic solution has a small thickness along which the reaction can propagate, and a comparatively large area. The time τ_f then essentially measures the initiation of the polymerization upon contact with anions. This explains why, for a given glue, increasing the Lipiodol concentration increases τ_f : the initiation of polymerization takes more time because there are less monomer molecules available. For any concentration, the polymerization time is shorter for pure nBCA glue than for Glubran 2 (Table 3), thus indicating that the functional monomer MS leads to an increase in the polymerization time of the glue.

SEM micrographs of the film surface are shown in Figure 17. For pure Glubran 2, the film structure (Figure 17a) is analogous to the one observed for the volume polymerization in the bulk (Figure 14a). However, in the case of glue-oil mixtures, the process is different: the mixture undergoes phase separation upon contact with the aqueous ionic solution. The tensioactive glue molecules are now located on the surface of the oil droplets. When the glue polymerizes, it encapsulates the oil droplets in a manner which is analogous to the procedure used to produce cyanoacrylate nanocapsules for drug transport [8]. The spectroscopic analysis of the white spherical particles in Figure 17b indicates the presence of iodine, and thus of Lipiodol. The defects that are observed on the surface of the film (Figure 16a) are probably due to the damage of encapsulated oil droplets during the removal of the film from the tube. Note that this phase separation/encapsulation process does not occur in the glue mixture volume, because there is no direct contact between the oil and the aqueous solution except at the tube wall.

4. Discussion and conclusion

We have conducted an *in vitro* study to quantitatively investigate the physical properties and the polymerization process of cyanoacrylate glues mixed with Lipiodol at various concentrations, Lipiodol being added to make them radio-opaque. Two glues have been investigated: Histoacryl, which is a pure nBCA glue, and Glubran 2, which is composed of nBCA and metacryloxysulpholane. We have confirmed that glue and Lipiodol are miscible. The addition of Lipiodol has the effect of modifying the physical properties of the glue: the viscosity, density and interfacial tension of the mixture with water all increase with the relative concentration in Lipiodol.

The experimental setup allows to rigorously investigate the glue polymerization when it is brought in contact with an anionic solution, analogous to

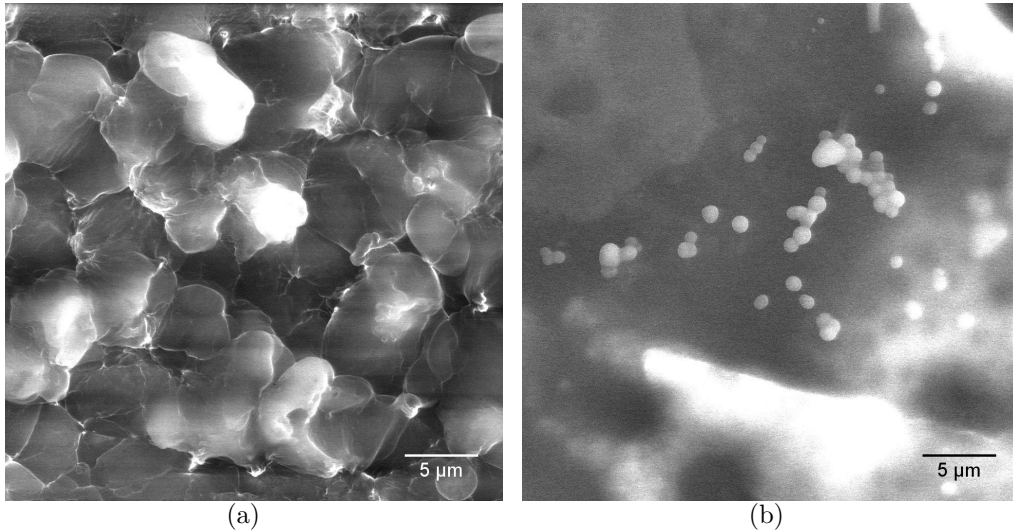


Figure 17: Scanning electron micrograph of the film surface: (a) pure Glubran, (b) G-L mixture ($C_G = 50\%$) where encapsulated oil droplets appear on the surface.

blood. The principle of the technique relies on the formation of a well-defined interface between the two liquids and on an objective measurement of the progression of the polymerization reaction by means of a high-speed imaging system, which measures the grey level change in the system. The results are very reproducible.

Various studies have reported on the polymerization mechanisms of nBCA under different experimental conditions [20, 21, 22]. They indicate that there are three distinct mechanisms whereby polymerization of pure nBCA may be initiated: anionic polymerization initiated by simple anions (acetate, hydroxide, cyanide, ...), zwitterionic polymerization initiated by covalent organic bases (either weak ones such as alcohol and amine, or strong ones such as triethylamine or pyridine), radical polymerization initiated by radicals. But in practice, the two favored modes are anionic and zwitterionic under classical experimental conditions. Hydroxide ions have been shown to provide optimal conditions for polymerization among all possible anions [23, 24]. As for Glubran 2, Levrier *et al.* [25] briefly mentioned in the introduction that the Glubran 2 polymerization pathway is radical contrary to pure nBCA, but none of the studies provided as references were conducted on the nBCA-MS monomers. It is, thus, difficult to know from the literature the exact mechanism responsible for the polymerization of Glubran 2.

We find that there is an initial polymerization phase, which is first very fast, since a 24- μm film is almost completely polymerized (and solidified) in 1 to 2 min depending on glue concentration. The polymerization of the mixture starts seconds after contact with the ionic solution and occurs at the interface between the two liquids. We confirm that the initial polymerization time increases with the proportion of Lipiodol, as was also found in previous studies with other methods [10, 11, 26]. This increase might be caused by the screening effect of oil molecules, which lowers the contact probability between the glue and anions. However, for nBCA-oil mixtures with $C_G = 50\%$, these previous studies report polymerization times between 3 s and 9 s, which are significantly smaller than the ones we measure ($\tau_f \sim 86$ s). The discrepancy may be due to the rather imprecise way the polymerization was assessed (change of opacity) in those studies and to the ionic fluid used (foetal veal serum, usually). Indeed, Figure 15 shows clearly that there is a fast drop in opacity during the first 10 s of contact, which is followed by a slower process as the reaction progresses inside the film. The differences in grey levels of the images in Fig. 15a for $t \geq 10$ s are not measurable with the naked eye and it takes a good imaging system to detect them.

Once the reaction is initiated, the glue mixture gradually polymerizes in volume, leading to the propagation of a polymerization front along the tube axis. This propagation process is slow and can take between 10 to 60 min for a 0.5 mm progression, the shortest time occurring for pure Glubran 2. Note that, for pure Histoacryl, the propagation over 0.5 mm takes only 3 min, which is extremely fast. During volume propagation, the initiated polymer chain increases by successively adding monomer molecules. Owing to this process, the intermolecular van-der-Waals forces convert to covalent bonds [27]. This results in a volume reduction and a density increase. Monitoring the volume shrinkage, or equivalently the change in length of the glue mixture, can thus be a simple alternative to the grey level analysis. As expected, the shrinkage increases with glue concentration (Figure 13). Indeed, the addition of Lipiodol increases the dilution of monomer molecules and increases both the polymerization half time and the shrinkage of the volumetric polymerization. Note that Glubran 2 results from the addition of a MS group to nBCA molecules, in order to slow down the polymerization process. Our results confirm that this objective is reached for pure glue (100%), but that the effect is inverted or not very important when the glue is mixed with Lipiodol (Figure 10).

For the sake of completeness, we have also tested very dilute mixtures

of Glubran or Histoacryl with Lipiodol, $C_G = 25\%$, a concentration that is sometimes used by surgeons for embolization. The vertical setup of Figure 5 could not be used as such in this case, since the glue mixture is denser than the ionic solution (see Figure 2): the configuration would have been prone to a Rayleigh-Taylor instability. The experiment was thus conducted in a horizontal tube. No measurable grey level change could be obtained within the glue mixture, which remained liquid for days after the experiment was stopped. This proves that it is very difficult for the polymerization to propagate within the glue volume when the concentration is as low as $C_G = 25\%$ in the case of an anionic initiation of the reaction. A polymerization reaction, however, occurred at the interface between the glue mixture and the ionic solution in the tube cross-section and led to the formation of a film of solidified glue: its existence was verified by introducing a wire into the tube. A thin film of glue was also left along the tube wall, which led to a grey level change in the ionic solution, as discussed previously (see section 3.3). The corresponding time constant of the film polymerization was found to be $\tau_f = 123$ s, which is consistent with the results of Table 3. We conclude that, for $C_G = 25\%$, the polymerization only occurs over micron scale distances and is slow.

All the present findings provide interesting results to interventional radiologists, who use Glubran 2 and Histoacryl as liquid embolic adhesives for vascular embolization. The glues are rarely used pure, because of the necessity to visualize their propagation in the vascular network and because of their very fast rate of polymerization on contact with anions. They are mixed with the radio-opaque Lipiodol oil, which, we have shown, modifies the time constants of polymerization: it results in a lengthening of the polymerization time and thus in a safer use of the mixture for embolization. To prevent premature polymerization in the micro-catheter or its blockage in the vessel during glue injection, clinicians tend to use glue concentrations $C_G \leq 50\%$. Our study shows that there is then a trade-off between delayed interfacial polymerization and full volume solidification. The hydrodynamic stresses exerted by blood circulation could well break up the droplets of injected glue at the early stages of their formation and prevent them from reaching the targeted site [28]. It is thus of paramount importance to study the interaction between injection hydrodynamics and glue polymerization, and extend the two-fluid injection study previously conducted on non-reacting liquids [13].

Conflict of Interest

The authors confirm that there are no known conflicts of interest associated with this publication and there has been no significant financial support for this work that could have influenced its outcome.

Acknowledgements

The authors would like to acknowledge the support from the Chinese Scholarship Council (for Y. J. Li's PhD fellowship). They thank GEM S.r.l. and Guerbet for having provided some Glubran 2 and Lipiodol samples, T. Delpech for his contribution to the characterization of the volumetric polymerization and Frédéric Nadaud (SAPC, Université de technologie de Compiègne) for the SEM pictures.

References

- [1] R. J. Rosen, S. Contractor, The use of cyanoacrylate adhesives in the management of congenital vascular malformations, *Seminars in Interventional Radiology* 21 (2004) 59 – 66.
- [2] S. K. Sarin, A. K. Jain, M. Jain, R. Gupta, A randomized controlled trial of cyanoacrylate versus alcohol injection in patients with isolated fundic varices, *American Journal of Gastroenterology* 97 (2002) 1010–1015.
- [3] L. Raffi, L. Simonetti, P. Cenni, M. Leonardi, Use of Glubran 2 acrylic glue in interventional neuroradiology, *Neuroradiology* 49 (2007) 829 – 836.
- [4] N. Bellemann, U. Stampfl, C. M. Sommer, H. U. Kauczor, P. Schemmer, B. A. Radeleff, Portal vein embolization using a Histoacryl/Lipiodol mixture before right liver resection, *Digestive Surgery* 29 (2012) 236 – 242.
- [5] L. Montanaro, C. R. Arciola, E. Cenni, G. Ciapetti, F. Savioli, F. Filippini, L. A. Barsanti, Cytotoxicity, blood compatibility and antimicrobial activity of two cyanoacrylate glues for surgical use, *Biomaterials* 22 (2001) 59 – 66.

- [6] V. Lenaerts, P. Couvreur, D. Christiaens-Leyh, E. Joiris, M. Roland, B. Rollman, P. Speiser, Degradation of poly (isobutyl cyanoacrylate) nanoparticles, *Biomaterials* 5 (1984) 65–68.
- [7] P. Maincent, R. L. Verge, P. Sado, P. Couvreur, J. P. Devissaguet, Disposition kinetics and oral bioavailability of vincamine-loaded polyalkyl cyanoacrylate nanoparticles, *Journal of Pharmaceutical Sciences* 75 (1986) 955–958.
- [8] N. A. K. Fallouh, L. Roblot-Treupel, H. Fessi, J. Devissaguet, F. Puisieux, Development of a new process for the manufacture of polyisobutylcyanoacrylate nanocapsules, *International Journal of Pharmaceutics* 28 (1986) 125 – 132.
- [9] E. Mele, J. A. Heredia-Guerrero, I. S. Bayer, G. Ciofani, G. G. Genchi, L. Ceseracciu, A. Davis, E. L. Papadopoulou, M. J. Barthel, L. Marini, R. Ruffilli, A. Athanassiou, Zwitterionic nanofibers of super-glue for transparent and biocompatible multi-purpose coatings, *Scientific Reports* 5 (2015) 14019.
- [10] M. F. Brother, J. C. Kaufmann, A. J. Fox, J. P. Deveikis, n-butyl 2-cyanoacrylate–substitute for IBCA in interventional neuroradiology: histopathologic and polymerization time studies, *American Journal of Neuroradiology* 10 (1989) 777 – 786.
- [11] C. Takasawa, K. Seiji, K. Matsunaga, T. Matsuhashi, M. Ohta, S. Shida, K. Takase, S. Takahashi, Properties of n-butyl cyanoacrylate-iodized oil mixtures for arterial embolization: in vitro and in vivo experiments, *Journal of Vascular and Interventional Radiology* 23 (2012) 1215 – 1221.
- [12] M. J. Gounis, B. B. Lieber, A. K. Wakhloo, R. Siekmann, L. N. Hopkins, Effect of glacial acetic acid and ethiodized oil concentration on embolization with n-butyl 2-cyanoacrylate: an in vivo investigation, *American Journal of Neuroradiology* 23 (2002) 938 – 944.
- [13] M. C. Sandulache, P. Paullier, R. Bouzerar, T. Yzet, O. Balédent, A. V. Salsac, Liquid injection in confined coflow: application to portal vein embolization by glue injection., *Physics of Fluids* 24 (2012) 081902.

- [14] S. Bracard, J. M. Macho-Fernández, X. Wang, R. Anxionnat, L. Picard, Influence of temperature on embolisation with cyanoacrylate, *Interventional neuroradiology* 4 (1998) 301 – 305.
- [15] M. C. Sandulache, Caractérisation in vitro de la technique endovasculaire d’embolisation par colle chirurgicale, Ph.D. thesis, Université de Technologie de Compiègne (2011).
- [16] C. A. Spade, V. A. Volpert, On the steady-state approximation in thermal free radical frontal polymerization, *Chemical Engineering Science* 55 (2000) 641 – 654.
- [17] A. Heifetz, L. R. Ritter, W. E. Olmstead, V. A. Volpert, A numerical analysis of initiation of polymerization waves, *Mathematical and Computer Modelling* 41 (2005) 271 – 285.
- [18] F. P. Bretherton, The motion of long bubbles in tubes, *Journal of Fluid Mechanics* 10 (1961) 166 – 188.
- [19] K. J. Stebe, D. Barthès-Biesel, Marangoni effects of adsorption-desorption controlled surfactants on the leading end of an infinitely long bubble in a capillary, *Journal of Fluid Mechanics* 286 (1995) 25 – 48.
- [20] E. F. Donnelly, D. S. Johnston, D. C. Pepper, D. J. Dunn, Ionic and zwitterionic polymerization of n-alkyl 2-cyanoacrylates, *Journal of Polymer Science: Polymer Letters Edition* 15 (1977) 399 – 405.
- [21] C. Limouzin, A. Caviggia, F. Ganachaud, P. Hémerly, Anionic polymerization of n-butyl cyanoacrylate in emulsion and miniemulsion, *Micromolecules* 36 (2003) 667 – 674.
- [22] J. Nicolas, P. Couvreur, Synthesis of poly(alkyl cyanoacrylate)-based colloidal nanomedicines, *Wiley Interdisciplinary Reviews: Nanomedicine and Nanobiotechnology* 1 (2009) 111 – 127.
- [23] I. C. Eromosele, D. C. Pepper, Anionic polymerization of butyl cyanoacrylate by tetrabutylammonium salts, 1. initiation processes, *Micromolecular Chemistry and Physics* 190 (1989) 3085 – 3094.
- [24] I. C. Eromosele, D. C. Pepper, Anionic polymerization of butyl cyanoacrylate by tetrabutylammonium salts, 2. propagation rate constants, *Micromolecular Chemistry and Physics* 190 (1989) 3095 – 3103.

- [25] O. Levrier, C. Mekkaoui, P. H. Rolland, K. Murphy, P. Cabrol, G. Moulin, J. M. Bartoli, C. Raybaud, Efficacy and low vascular toxicity of embolization with radical versus anionic polymerization of n-butyl-2-cyanoacrylate (NBCA). an experimental study in the swine, *Journal of Neuroradiology* 30 (2003) 95 – 102.
- [26] L. D. Cromwell, C. W. Kerber, Modification of cyanoacrylate for therapeutic embolization: preliminary experience, *American Journal of Roentgenology* 132 (1979) 799 – 801.
- [27] M. Atai, D. C. Watts, Z. Atai, Shrinkage strain-rates of dental resin-monomer and composite systems, *Biomaterials* 26 (2005) 5015 – 5020.
- [28] F. Baltacıoğlu, N. C. Cimşit, K. Bostancı, M. Yüksel, N. Kodalli, Transarterial microcatheter glue embolization of the bronchial artery for life-threatening hemoptysis: Technical and clinical results, *European Journal of Radiology* 73 (2010) 380 – 384.